

Electronic structure of the organic conductor α -(BEDT-TTF) $_2$ I $_3$ studied by angle-resolved and core-level photoelectron spectroscopy

S. Söderholm

*Materials Physics, Department of Physics, Royal Institute of Technology, S-100 44 Stockholm, Sweden
and ABB Corporate Research, Department of Materials and Chemical Engineering, S-72178 Västerås, Sweden*

R. T. Girard

Materials Physics, Department of Physics, Royal Institute of Technology, S-100 44 Stockholm, Sweden

D. Schweitzer

3. Physikalisches Institut, Universität Stuttgart, Pfaffenwaldring 57, D-70550 Stuttgart, Germany

(Received 29 April 1996)

The electronic structure of the organic conductor α -(BEDT-TTF) $_2$ I $_3$ has been studied by photoelectron spectroscopy on *in situ* cleaved crystals. The valence-band regime consisted of eight distinct features with binding energies between 1.2 and 10.9 eV. Angle-resolved measurements showed no dispersion along the Γ -Z (k_z) direction, i.e., perpendicular to the conducting BEDT-TTF layers, for the structures in the valence-band regime. Angle-resolved measurements along the a and b axis, i.e., approximately along a^* and b^* , gave no evidence that the structures closest to the Fermi level show any dispersion in the highly conducting plane. The present experiment sets an upper limit for the dispersion of about 0.25 eV. The lack of any (observable) dispersion and the lack of a sharp Fermi edge in spite of α -(BEDT-TTF) $_2$ I $_3$ showing metallic transport properties are thoroughly discussed. It is argued that correlation effects or the calculated narrow-gap semiconductor band structure of α -(BEDT-TTF) $_2$ I $_3$ are the most probable explanations for the latter phenomena. From the photon energy dependence, the atomic origin of several structures in the valence-band regime is suggested. Core-level spectroscopy on the I 4*d* level revealed the presence of one bulk component and a surface shifted component. S 2*p* core-level spectra revealed no surface or chemically shifted components. The large width of the bulk components of these core levels is primarily ascribed to phonon broadening. [S0163-1829(97)01707-4]

I. INTRODUCTION

Organic conductors based on BEDT-TTF, where BEDT-TTF is an abbreviation for bis(ethylenedithio)tetrathiafulvalene, have attracted a lot of interest as the majority of the known organic superconductors and those with the highest critical temperature are based on BEDT-TTF.^{1,2} The charge-transfer (CT) complexes derived from BEDT-TTF have similar structures; they consist of alternating sheets of BEDT-TTF and anions. Several of the CT complexes have the same composition, but exist in different crystallographic phases with widely different physical properties; e.g., the α phase of (BEDT-TTF) $_2$ I $_3$ undergoes a metal-to-insulator transition at 135 K (Ref. 3) but the β phase has a superconducting ground state, $T_c \approx 1.5$ K.⁴ These facts make the (BEDT-TTF) $_2$ I $_3$ suitable for studies of the relationship between crystal structure and electronic properties. Although these molecular solids have been extensively studied, the knowledge of their electronic structure is sparse, and such knowledge is fundamental for understanding the intriguing properties of organic conductors and organic superconductors. Experimental difficulties have hampered the use of photoelectron spectroscopy as a tool for probing the electronic structure, since the samples have a small surface and are thin, and the technique requires a clean surface on the sample. On the other hand, the quasi-two-dimensional electronic structure of the BEDT-TTF based CT complexes makes them

suitable for angular-resolved measurements. The difficulties have been overcome by studying *in situ* grown films^{5,6} or by developing techniques for cleaving the samples *in situ*; by the latter technique crystals of some BEDT-TTF derived complexes have been studied.⁷⁻⁹

In this paper a comprehensive set of photoelectron spectroscopical data of α -(BEDT-TTF) $_2$ I $_3$ single crystals cleaved *in situ* are presented; angular-resolved normal emission photoemission spectra of the valence-band regime recorded with photon energies between 21 and 150 eV, angular-resolved photoemission spectra covering the Brillouin zone along approximately the k_a and k_b directions, and core-level spectra of S 2*p* and I 4*d*. Details about the transport properties of α -(BEDT-TTF) $_2$ I $_3$ are given in Refs. 1-3. The unit cell is described by $a=9.211$ Å, $b=10.850$ Å, $c=17.488$ Å, $\alpha=96.95^\circ$, $\beta=97.97^\circ$, and $\gamma=90.75^\circ$.¹⁰

II. EXPERIMENT

The photoemission experiments were performed at the toroidal grating monochromator beamline at the MAX-lab, the national synchrotron radiation laboratory in Lund, Sweden. The spectra were recorded with a goniometer-mounted hemispherical angle-resolving electron energy analyzer, acceptance $\pm 1^\circ$. For a comprehensive description of the beamline see Karlsson *et al.*¹¹ A thoroughly sputtered Ta foil in electrical contact with the sample was used as a reference for the

Fermi level, and from the width of the tantalum Fermi edge the total-energy resolution of the spectra, photon, and electron contributions, was determined. For the valence-band spectra the resolution was determined to be 0.25 eV at a photon energy of 21 and 0.35 eV at $h\nu=100$ eV, and 0.55 eV at $h\nu=180$ eV.

A comprehensive description of the cleavage of the single crystals and the design of the sample holder, to avoid any spurious signal from the holder due to the small size of the samples, is given in Ref. 7. The only difference was that the conducting Ag epoxy used to attach the crystals to the sample holder in this study cured at room temperature.

The samples used in the present study were electrochemically grown single crystals with areas between $\sim 3 \times 2$ and $\sim 2 \times 1$ mm². The surface of a cleaved crystal was smooth and had a black-brownish color. The crystals appear blacker if they are thicker. The surface of the cleaved crystal is not as shiny as the surface of as grown crystal, but rather looks more like an unpolished metal surface. It is evident from the crystal structure that the cleavage will occur between the weakly bonded BEDT-TTF and I₃⁻ layers.

The samples were carefully aligned by eye with the aid of the shape of the crystals, in order to avoid exposing the crystals to an electron beam, since it is well known that organic conductors are sensitive to irradiation, especially particle bombardment; see, for instance, Ref. 12. Several test spectra were recorded to ensure that the influence of the background (epoxy and sample holder) was negligible. In order to excite both orbitals in the plane of the surface and perpendicular to it the photon angle of incidence was 45°. No changes in the recorded spectra were detected during the measurements. The base pressure in the analysis chamber, where the crystals were cleaved, was $< 3 \times 10^{-10}$ mbar.

III. RESULTS AND DISCUSSION

Photoemission spectra of the valence-band regime of an α -(BEDT-TTF)₂I₃ crystal recorded in normal emission with different photon energies in the range 21–150 eV are shown in Fig. 1. The spectra in this figure are normalized to the same height in order to facilitate a comparison of how the relative intensity of the different structures varies with the photon energy, and to make visible as many of the structures in the different spectra as possible.

There are eight structures observable in the valence-band regime, labeled A–H in Fig. 1, these structures have binding energies (E_b) between 1.2 and 10.9 eV relative to the Fermi level, $E_F=0$. The determined binding energies for A–H are 1.2, 2.1, 3.4, 4.1, 5.7–6.0, 7.6, 9.6, and 10.9 eV. All of the structures except structure D are distinct and visible in all spectra. Structure D is seen as a weak peak or as a shoulder when the exciting photon energy is larger than 70 eV or below 25 eV. Figure 1 shows that all structures except E have binding energies that are independent of the exciting photon energy. The deviations of the binding energies of each of these structures from a constant value appear to be random and at the most 0.10–0.15 eV for a particular structure, i.e., well within the experimental resolution. The binding energy of structure E shows larger changes, and the change of binding energy with photon energy does not seem to be random. The gradual change of shape of this peak

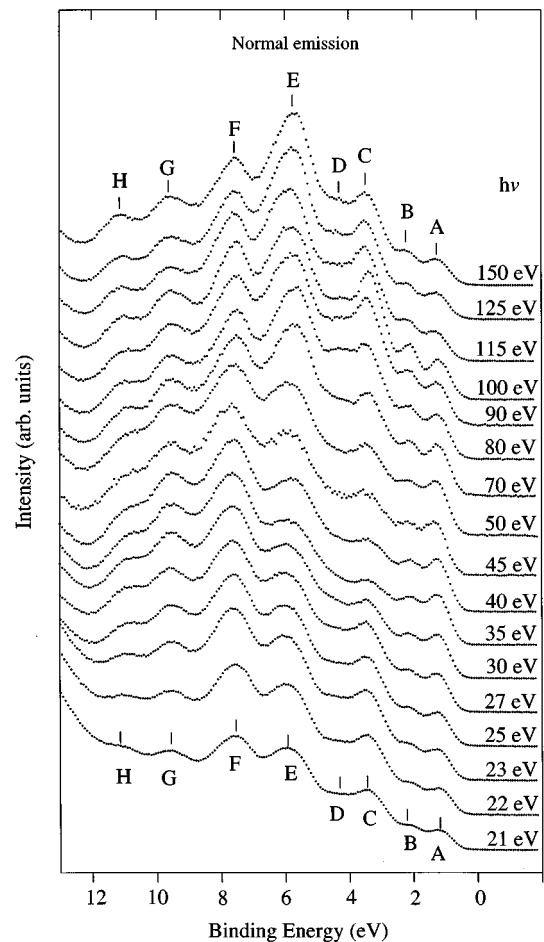


FIG. 1. Valence-band photoemission spectra of α -(BEDT-TTF)₂I₃ obtained in normal emission with photon energies between 21 and 150 eV. Different structures in the valence-band regime are labeled A to H and marked with tick marks in the spectra. The spectra are normalized to the same height.

when the photon energy is decreased from 150 to 50 eV together with the shift of peak position when the photon energy is decreased below 70 eV shows that this structure consists of two closely lying structures. At photon energies above 70 eV the structure with the lowest binding energy is dominating and the other structure is seen as a shoulder on the high binding energy side of the dominating structure. But, at lower photon energies the structure with the highest photon energy is dominating, and the other is not discernible at photon energies below 30 eV. Thus, the present investigation gives no support for dispersing bands in the Γ -Z (k_z) direction. The lack of dispersion in this direction is in agreement with the two-dimensional electronic structure of the BEDT-TTF salts deduced from galvanometric and optical measurements.¹

Since the wave vector parallel to the surface (k_{\parallel}) is conserved in photoemission, within a reciprocal lattice vector, a variation of the emission angle changes the value of k_{\parallel} . In a two-dimensional structure $k_{\parallel} = (2\pi/h)(2m_e E_k)^{1/2} \sin \theta$, where E_k is the kinetic energy of the emitted electron, and θ is the emission angle with respect to the surface normal, i.e., the polar angle. Thus if the azimuthal angle is kept constant the E_b versus k_{\parallel} relationship can be determined. In the

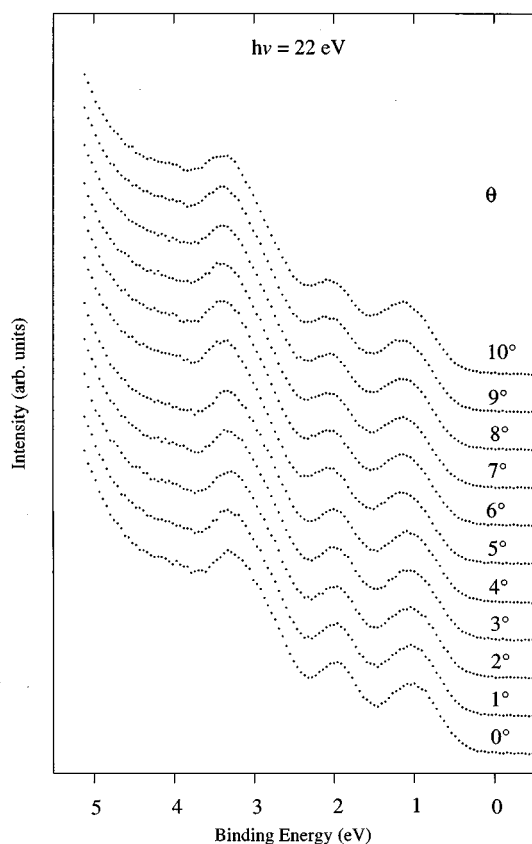


FIG. 2. Photoemission spectra of α -(BEDT-TTF) $_2$ I $_3$ along a , i.e., approximately along the ΓX azimuth, recorded with a photon energy of 22 eV. The spectra are normalized to the same height.

present study, the measurements were performed along the axis of the studied surfaces a and b , which are close to the principal directions a^* and b^* in reciprocal space. The angle between a and a^* (b and b^*) is 0.75° and the angle between the surface normal and a^* (b^*) is 82.03° (82.05°). The large crystallographic unit cell of α -(BEDT-TTF) $_2$ I $_3$ makes the first Brillouin zone small and because of the finite angular resolution of the analyzer the probed part of momentum space is roughly one-quarter of $a^*/2$ or $b^*/2$. Thus the performed measurements are not truly angle resolved. Figure 2 shows spectra, recorded at 22-eV photon energy, covering the part of the valence-band regime containing structures A – D measured along the a direction. An emission angle of 0° corresponds to the Γ point, and an emission angle of about $\theta=10^\circ$ corresponds to the X point ($a^*/2,0,0$). The corresponding set of data obtained along the b direction is shown in Fig. 3. In this figure the Y point ($0,b^*/2,0$) corresponds to an emission angle of about $\theta=8^\circ$. It is clear from these figures that the present investigation gives no evidence that the structures closest to the Fermi level show any dispersion in the highly conducting plane.

Since no dispersion could be detected in the present experiment an upper limit for the dispersion can be established. The experimental details imply that any dispersion is less than 0.25 eV. Thus, if the bands, formed by molecular orbitals, that give rise to structures A , B , and C are dispersing the dispersion is less than about 0.25 eV. The dispersion might be slightly larger if the structures are due to two or more

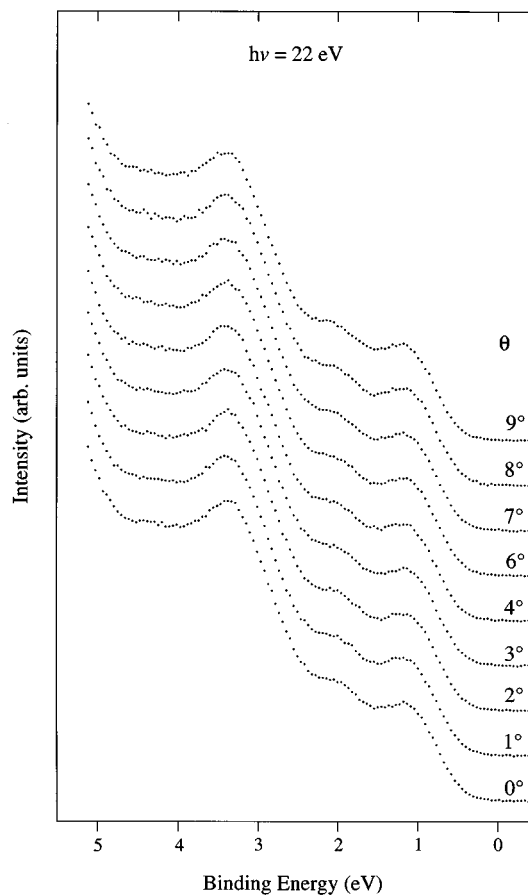


FIG. 3. Photoemission spectra of α -(BEDT-TTF) $_2$ I $_3$ along b , i.e., approximately along the ΓY azimuth, recorded with a photon energy of 22 eV. The spectra are normalized to the same height.

closely lying features, as in C_{60} where a high-resolution photoemission study together with numerical fits were needed in order to observe any dispersion in the bands formed by the highest occupied molecular orbitals (HOMO).¹³ However, it is clear that the bands in α -(BEDT-TTF) $_2$ I $_3$ are rather flat, in agreement with the fact that the electronic structure of a molecular solid is primarily governed by the electronic structure of the different molecules forming the solid, at least when the solid consists of distinct molecular species. This is ascribed to the fact that molecular solids are mainly held together by weak van der Waals forces. Firm experimental evidence for this is given by a comparison of photoemission spectra of the gas phase and the solid; the main difference is that the bands in the spectrum of the solid are broadened and rigidly shifted in comparison with the gas-phase spectrum.^{14–17} Even in the case of charge-transfer complexes features in the valence band can be traced back to bands in the gas-phase spectra^{5,15} and/or in the spectrum of the neutral donor (or acceptor).¹⁸ The preservation of the molecular origin in the case of BEDT-TTF has been thoroughly shown and discussed in Refs. 5 and 7, and is also evident from a comparison of the binding energies of the structures in the valence band in different CT complexes based on BEDT-TTF,⁹ which in addition are similar to the binding energies in the present case. Thus, the lack of any observable dispersion is in agreement with the ‘‘molecular nature’’ of α -(BEDT-TTF) $_2$ I $_3$.

The different contributions to width of the structures, besides the possibility of several components (as discussed above), can be divided into two parts, i.e., the experimental resolution and intrinsic mechanisms. The energy resolution has been reported in the experimental section. The contribution from a finite k resolution will be small as the bands are flat. Of the intrinsic effects the lifetime broadening is expected to small since the structures in the valence band are situated fairly near the Fermi level. But, a large contribution from phonon broadening is in agreement with organic conductors being “soft materials,” and experimental data from C_{60} where the phonon broadening was determined to 0.3–0.4 eV.¹⁹ Molecular solids are “soft materials” in the sense that many phonons are excited at room temperature, and the large number of atoms in the unit cell makes many phonon modes possible. In organic compounds the thermal motion of the atoms causes the root-mean-square value of the displacement, as determined by x-ray diffraction experiments, to be up to 0.5 Å. This value is typically 0.05–0.10 Å in inorganic compounds.²⁰ The above facts together with the widths of the structures in the valence band imply that phonon broadening is the main contribution.

In spite of the metallic properties observed in galvanometric experiments¹ no sharp Fermi edge is seen at any of the investigated points in the first Brillouin zone, see Figs. 1, 2, and 3. A finite spectral intensity is seen within about 250 meV from E_F , with the present energy resolution the onset of the intensity cannot be determined more accurately. Among the organic conductors studied by photoelectron spectroscopy, i.e., TTF-TCNQ and other TCNQ compounds,^{15,21} (DCNQI)₂X salts,^{22–28} (TMTSF)₂PF₆,²⁹ and different (BEDT-TTF)₂X salts,^{5,7,8,9} only in the case of (DMe-DCNQI)₂Cu a sharp Fermi edge has been observed.^{22–24} However, other groups do not observe a sharp Fermi edge in the spectra of (DMe-DCNQI)₂Cu,^{27,28} even if the samples were prepared and handled in a similar way. In all other cases a small band gap was observed or an onset of spectral intensity almost at the Fermi level was seen. It has been proposed that the absence of a Fermi edge is caused by the surface sensitivity of photoelectron spectroscopy in combination with the surface being insulating. But from the considerations and experimental data put forward in Refs. 5, 7, and 8 this explanation seems unlikely.

In the first reports of photoelectron spectroscopy studies of organic conductors^{15,21} the lack of a sharp Fermi edge was explained by the excitations of high-energy phonons in the photoemission process that should shift the emission to higher binding energies and broaden the spectral features. However, a recent photoemission study by Dardel *et al.* of metallic systems with different dimensionality³⁰ strongly suggested that this particularity was associated with materials with a one-dimensional electronic structure, in which the presence of strong electron-electron correlations causes the system to be a Luttinger liquid; i.e., there is no discontinuity in the momentum distribution at the Fermi level and the electronic spectral function vanishes at E_F .³¹ An alternative explanation was proposed by Purdie *et al.*, who suggested that the lack of spectral intensity at E_F was due to a fluctuating charge-density wave (pseudogap).³² This interpretation cannot be a general one since studies of two-dimensional materials undergoing a metal-semiconductor transition^{33,34}

and on one-dimensional materials^{29,35–37} support that correlation effects are the most probable cause to the absence of a sharp Fermi edge in one-dimensional electronic systems. Especially the studies of (TMTSF)₂PF₆ and BaVS₃ give strong evidence for this since the e - e interaction is much stronger than the electron-phonon interaction in (TMTSF)PF₆ (Ref. 29) and in BaVS₃ where the opening of a band gap was observed around the transition temperature for the metal-semiconductor transition.³⁶ Thus, the most probable explanation for the lack of a sharp Fermi edge in the above-mentioned organic conductors, except the BEDT-TTF based ones, is the presence of correlation effects in a one-dimensional electronic structure. In the case of the BEDT-TTF based organic conductors several plausible explanations exist.

Since experimental data suggest that the excitation of phonons is not the dominating mechanism behind the lack of a sharp Fermi edge in quasi-one-dimensional organic conductors, it is likely that this mechanism is not a proper explanation in two-dimensional organic conductors. On the other hand it is accepted that the molecular origin gives rise to appreciable correlation effects and narrow bands in organic conductors; see, for instance, Refs. 1, 38, and 39. In this case the absence of quasiparticle excitations should be caused by the formation of a two-dimensional Luttinger liquid. It has recently been proposed that Luttinger liquid theory might be valid in two dimensions⁴⁰ and shown that an excitation spectrum corresponding to a two-dimensional Luttinger liquid can be obtained in specific situations.^{41–44}

The fulfillment of these requirements in the BEDT-TTF based organic conductors might distinguish them from the other two-dimensional materials, which show a Fermi edge, e.g., layered metal chalcogenides. In this context it should be noted that both experimental data (mainly Shubnikov–de Haas and de Haas–van Alphen experiments) (see, for instance, Refs. 45–48) and theoretical calculations of the electronic structure (see, for instance, Refs. 49–52) have given evidence for the presence of both closed hole pockets and open electronlike Fermi surfaces in some BEDT-TTF salts. The latter is a Fermi surface similar to the Fermi surface of a quasi-one-dimensional material, which could cause the material to behave in a one-dimensional way, i.e., causing the material to be a one-dimensional Luttinger liquid. (It has been shown that if the exponent giving the asymptotic power law of the spectral function for a one-dimensional Luttinger liquid is large the momentum resolved spectral features will not show any significant dispersion.⁵³)

Band-structure calculations have been performed for some BEDT-TTF based materials and give another possible explanation for the lack of a sharp Fermi edge in some cases since they predict a low density of states at E_F for β -(BEDT-TTF)₂I₃,⁹ and that α -(BEDT-TTF)₂I₃ is a narrow-gap semiconductor.^{54,55} The tight-binding calculations of the band structure of α -(BEDT-TTF)₂I₃ by Emge *et al.*⁵⁴ employed both single- and double-zeta Slater type. Both calculations gave similar results for the four bands derived mainly from the HOMO of the BEDT-TTF molecule; i.e., these bands span a narrow energy range of 0.3 and 0.7 eV, respectively, all bands are narrow, and the bandwidth is less than 100 meV. The single- ζ basis calculation predicts a direct band gap of 13 meV at Y (double ζ : indirect band gaps of

about 100 meV) and a maximum dispersion along the Γ - Y and X - M directions. At room temperature the Fermi surface would consist of small electron pockets around the Y point. [However, since the calculated bands are very narrow the presence of significant correlation effects would strongly affect the electronic structure of α -(BEDT-TTF) $_2$ I $_3$.] Thus, the predicted band structure is in qualitative agreement with the recorded valence-band spectra; i.e., the dispersion is too small to be detected and structure A may consist of unresolved structures, and the presence of spectral intensity up to the Fermi level is due to excitation of electrons to the conduction band. In this case the absence of a Fermi edge from the degenerate semiconductor can be ascribed to a low electron density in the conduction band of α -(BEDT-TTF) $_2$ I $_3$, since the electron density in an organic conductor is a factor 10–100 smaller than in ordinary metals. An additional cause can be a low probability for photoelectron excitations in α -(BEDT-TTF) $_2$ I $_3$. Thus, it is suggested that correlation effects or the predicted narrow-band-gap semiconductor structure are the most likely reasons for the lack of a finite spectral intensity at the Fermi level in α -(BEDT-TTF) $_2$ I $_3$.

By comparing the relative intensities of the structures in the valence-band regime information about the atomic character of the molecular orbitals associated with the structure can be obtained. In order to avoid influences of final-state effects in the sense that the final state is not well described by a free-electron-like state the emphasis will be on spectra recorded with a photon energy higher than 30–35 eV; in this regime the background is low, which also facilitates the analysis. The most striking change of relative intensity seen in Fig. 1 is that structure F has the highest intensity below 50 eV but above 70 eV structure E dominates the spectra. Clear intensity variations are also shown by structure C , which appears to have a minimum around 30–35 eV and a maximum around 90 eV. A careful inspection of the different spectra shows that the intensities of structures A and B decrease faster than the intensities of G and H when the photon energy is increased. Structures A and B appear to have a weak and broad maximum in their intensities around 40–45 eV. From these observations together with the calculated atomic cross sections of C $2s$, C $2p$, S $3s$, and S $3p$ (Ref. 56) some knowledge of the atomic origin of the different structures can be extracted. The calculated cross sections show that for photon energies above 50 eV the cross sections for C $2s$ and C $2p$ decrease faster with increasing photon energy than the cross sections for S $3s$ and S $3p$; this suggests that structures A and B have mainly carbon character but structures G and H have dominant sulfur character. The presence of a clear minimum and a clear maximum in the relative intensity of structure C implies that this structure is derived from S $3p$ orbitals, since this orbital is the only one that displays such a behavior of the cross section. The facts that structure E becomes dominant at high photon energies and that its relative intensity increases rapidly in the photon energy regime between 50 and 70 eV strongly suggest that structure E has S $3p$ character, even if the presence of a minimum in the intensity is not clearly seen at low photon energies. The shift of the strongest feature from F to E between 50 and 70 eV, together with the observation that structures G and H increase in intensity relative to F , for photon energies higher than 70 eV gives support for structure F

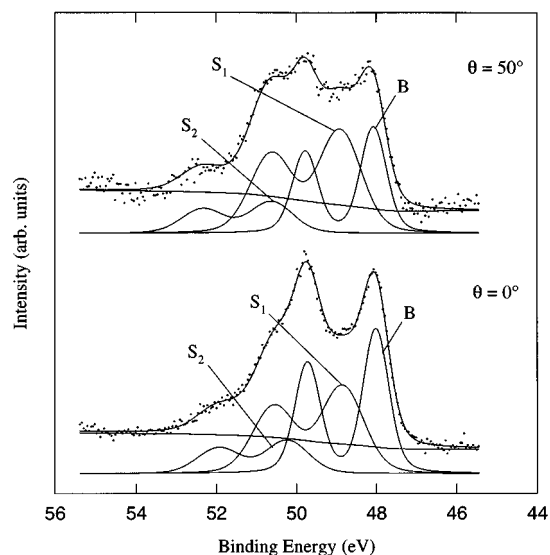


FIG. 4. I 4d core-level spectra, excited with a photon energy of 180 eV. The points represent the experimental data, recorded at different emission angles; bottom 0° , top 50° . The full lines are the result of a curve fitting procedure. The parameters used are given in the text. The spectra are normalized to the same height.

having dominant C $2p$ character, since the calculated cross sections predict that the cross section of C $2p$ is the largest one at a photon energy of 40 eV but S $3p$ has the largest cross section at 70 eV and the cross section of C $2p$ is decreasing faster than the other when the photon energy is increased.

The present data give no support for the intensity variations being due to critical points in the Brillouin zone since if this were the case the relative intensities would display a periodic behavior, and with reasonable choices of the inner potential at least two maximum (or minimum) would appear in the present photon energy regime.

Two shallow core levels (inner valence states) were observed close to the valence band regime. It is not clear to which extent the two observed levels mix with the valence band or if they are a part of it. These levels had binding energies of 13.8 and 18.2 eV, and the recorded structures were broad. Their full widths at half maximum (FWHM) were about 2 and 4 eV, respectively. The state with the lowest binding energy gives rise to the upturn of the spectra in Fig. 1 at the highest binding energies. The fact that shallow core levels have been observed in the same binding energy range in other BEDT-TTF based salts and in other organic conductors, with and without sulfur,^{5–7,9,18,57–59} has been used to associate the structure with $E_b \approx 13$ –14 eV with C $2s$ σ -type orbitals.⁷ The structure with $E_b \approx 18$ eV observed in BEDT-TTF salts^{5,7,9} cannot be unambiguously assigned; it could either originate from S $3s$ or C $2s$ orbitals or be due to many-body effects.⁵⁹

The I 4d core level was recorded at two different emission angles, 0° and 50° , as shown in Fig. 4. The count rate was very low during these measurements, each spectrum was recorded during the lifetime of the electron beam injected into the storage ring, i.e., 3–4 h. Even if the noise level is rather high in the displayed spectra it is clear from the shape

of spectra that it consists of several components, and that one component decreases in intensity when the measurement is more surface sensitive; i.e., the emission angle is increased. In order to extract more information from the spectra they were fitted to a simulated line shape, which was obtained through a convolution of a Lorentzian and a Gaussian function. The latter simulates broadening of the spectrum due to the resolution of the apparatus, phonons, and disorder. The former represents the limited lifetime of the core hole created by the excitation. To obtain a good fit it was necessary to use three doublets, labeled *B*, *S1*, and *S2* (see Fig. 4). The doublets had a Lorentzian FWHM of 0.20 eV, a spin-orbit splitting of 1.71 eV, and a branching ratio of 1.30. From the fitting procedure a binding energy of 47.9 eV and a Gaussian FWHM of 0.65 eV for component *B* were obtained. The components *S1* and *S2* were found to have binding energies of 48.8 and 50.1 eV and a Gaussian FWHM of 1.15 eV.

The shape of the spectra recorded at different emission angles and the belonging fits show that doublet *B* is a bulk feature and that *S1* and *S2* are associated with iodine on the surface. A tentative assignment is that *S1* is due to I_3^- on the surface, and that *S2* is due to iodine associated with steps and other imperfections on the surface. The latter assignment is based on the fact that the tail on the high binding energy side of the spectrum was pronounced and extended on samples with an inferior surface quality, as viewed by the eye. From the present data no conclusions can be drawn about the chemical state of this kind of iodine. This assignment of the different components is in agreement with the different Gaussian widths; since only small amounts of iodine are present on the surface it is very likely that the components *S1* and *S2* are broadened in comparison with *B* due to the influence of disorder. The low count rate of *B*, due to I_3^- in the bulk, is caused by the fact that the first I_3^- layer is situated about 17 Å below the surface and because the elastic mean free path of photoelectrons is shorter than this distance the signal is severely attenuated. The present data suggest that the elastic mean free path as a function of kinetic energy in organic materials cannot be widely different from the relation in metals and semiconductors; for a comprehensive discussion see Ref. 14. The weak signal from the iodine on the surface shows that only a very small amount of iodine is present on the surface. This was the case for all studied crystals. From the results of scanning tunneling microscopy studies of α -(BEDT-TTF) $_2$ I $_3$ (Ref. 60) and β -(BEDT-TTF) $_2$ I $_3$ (Ref. 61), which revealed no iodine on the surface of the crystals, it has been suggested that the lack of iodine on the studied surfaces could be due to an inherent instability of the I_3^- layer. However, the fact that the binding energy of the I 4*d* level in *c*-axis-oriented thin films of α -(BEDT-TTF) $_2$ I $_3$ [hereafter abbreviated α_f -(BEDT-TTF) $_2$ I $_3$] was 48.9 eV, i.e., in excellent agreement with the binding energy of the surface component *S1* in α -(BEDT-TTF) $_2$ I $_3$, implies that the I 4*d* signal observed from α_f -(BEDT-TTF) $_2$ I $_3$ and α_t -(BEDT-TTF) $_2$ I $_3$ crystals originates from the surface, not from the bulk as previously suggested.^{5,7} Further support for this reassignment is given by the high intensity from I 4*d* in α_f -(BEDT-TTF) $_2$ I $_3$ and α_t -(BEDT-TTF) $_2$ I $_3$, which in the light of the low intensity from the bulk in α -(BEDT-TTF) $_2$ I $_3$ indicates that a strong I 4*d* signal can only arise from large

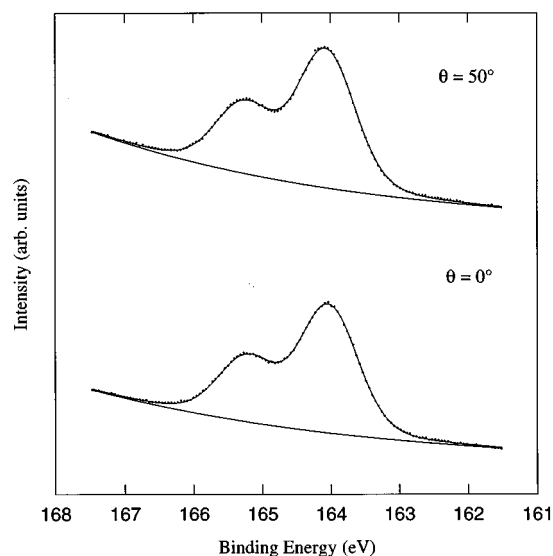


FIG. 5. S 2*p* core-level spectra, excited with a photon energy of 180 eV. The points represent the experimental data, recorded at different emission angles; bottom 0°, top 50°. The full lines are the result of a curve fitting procedure. The parameters used are given in the text. The spectra are normalized to the same height.

amounts of iodine on the surface. Thus, the I_3^- layer is not always unstable.

A comparison of the Gaussian FWHM used in the fits of the data from α -(BEDT-TTF) $_2$ I $_3$, α_f -(BEDT-TTF) $_2$ I $_3$ (~0.95 eV) (Refs. 5 and 6) and α_t -(BEDT-TTF) $_2$ I $_3$ (~0.80 eV) (Ref. 7) shows that the surface components are significantly larger than the only observed bulk component, i.e., component *B* in the α -(BEDT-TTF) $_2$ I $_3$ spectrum. The present investigation suggests that this is mainly due to a larger contribution from disorder, and that the influence of disorder on the linewidth is increased when the amount of I_3^- (and other iodine species) on the surface is small. The width of the bulk component can be ascribed to phonon broadening. A fairly large phonon-induced linewidth is consistent with organic conductors being “soft materials.”

The S 2*p* spectrum can be reproduced well by fitting with one doublet, giving a binding energy of 163.9 eV for the S 2*p* $_{3/2}$ level. In this fit a spin-orbit splitting of 1.20 eV, a branching ratio of 2.03, a Lorentzian FWHM of 0.20 eV, and a Gaussian FWHM of 0.89 eV were used; see Fig. 5. It should be noted that the spectra can be fitted equally well by using two components if the Gaussian FWHM is set to about 0.7 eV. These components have almost equal intensities, and the intensity ratio is nearly the same for the investigated emission angles. As the measured S 2*p* spectra give no clear support that the spectrum consists of more than one component, i.e., no shoulders are seen, spectra recorded at different emission angles are congruent etc., a fit with one component is shown in Fig. 5. Since the core-level spectrum of S 2*p* in α_t -(BEDT-TTF) $_2$ I $_3$ could be fitted with the same Gaussian FWHM (Ref. 7) it is suggested that phonon broadening governs the width of the S 2*p* core level. It is very likely that the influence on the S 2*p* level from the presence of a fairly ordered I_3^- layer or from disordered patches of I_3^- does not give rise to any noticeable changes, since the sulfur atoms closest to the surface are found some Å below it, and, fur-

thermore, the electronic interaction perpendicular to the BEDT-TTF layer is weak because of the two-dimensional electronic structure of the BEDT-TTF salts deduced from galvanometric and optical measurements.¹

IV. SUMMARY

The electronic structure of the organic conductor α -(BEDT-TTF)₂I₃ has been studied by photoelectron spectroscopy on *in situ* cleaved crystals. The valence-band regime consisted of eight distinct features with binding energies between 1.2 and 10.9 eV. Angle-resolved measurements showed no dispersion along the Γ -Z (k_z) direction, i.e., perpendicular to the conducting BEDT-TTF layers, for the structures in the valence-band regime. Angle-resolved measurements along the a and b axes, i.e., approximately along a^* and b^* , gave no evidence that the structures closest to the Fermi level show any dispersion in the highly conducting plane. The present experiments sets an upper limit for the dispersion of about 0.25 eV. The lack of any dispersion and the lack of a sharp Fermi edge in spite of α -(BEDT-TTF)₂I₃ showing metallic transport properties was thoroughly discussed. It was argued that correlation effects or the calculated narrow-gap semiconductor band structure of α -(BEDT-TTF)₂I₃ are the most probable explanations for the latter phenomena.

The changes of the shape of the valence-band spectrum when the photon energy was changed together with calculated cross sections for atomic orbitals made it possible to

determine the atomic origin of several structures in the valence band. The two structures closest to the Fermi level have mainly carbon character and the third is mostly derived from S $3p$ orbitals, as the fifth structure.

Two shallow core levels (inner valence states) with binding energies of 13.8 and 18.2 eV were observed. The former is most likely due to C $2s$ σ -type orbitals. The latter cannot be unambiguously assigned. The I $4d$ and the S $2p$ core levels were also studied.

The I $4d$ signal was very weak since it consisted of one component from the bulk, since the I₃⁻ layer closest to the surface is situated about 17 Å below the surface, two components that could be ascribed to iodine on the surface were also observed. These were ascribed to small patches of I₃⁻ on the surface and to iodine associated with steps and other imperfections on the surface. The surface component was shifted 0.9 eV in comparison with the bulk component, $E_B=47.9$ eV. The S $2p$ spectrum could be fitted with one component, i.e., no surface or chemically shifted components were detected. It was argued that the large width of the I $4d$ bulk component and the S $2p$ core level can be ascribed to phonon broadening, since organic conductors are "soft materials" in the sense that many phonons are excited at room temperature, and that many phonon modes are possible due to the large number of atoms in the unit cell.

ACKNOWLEDGMENT

R.T.G. is grateful to the Swedish Natural Science Research Council (NFR) for financial support.

- ¹T. Ishiguro and K. Yamaji, *Organic Superconductors* (Springer, Berlin, 1990), Chap. 5.
- ²J. M. Williams, A. J. Schultz, U. Geiser, K. D. Carlson, A. M. Kini, H. H. Wang, W.-K. Kwok, M.-H. Whangbo, and J. E. Schirber, *Science* **252**, 1501 (1991); J. M. Williams, J. R. Ferraro, R. J. Thorn, K. D. Carlson, U. Geiser, H. H. Wang, A. M. Kini, and M. H. Whangbo, *Organic Superconductors* (Prentice Hall, Englewood Cliffs, NJ, 1992).
- ³K. Bender, I. Hennig, D. Schweitzer, K. Dietz, H. Endres, and H. J. Keller, *Mol. Cryst. Liq. Cryst.* **107**, 359 (1984); I. Hennig, K. Bender, D. Schweitzer, K. Dietz, H. Endres, H. J. Keller, A. Gleitz, and H. W. Helberg, *Mol. Cryst. Liq. Cryst.* **119**, 337 (1985).
- ⁴E. B. Yagubskii, I. F. Shchegolev, V. N. Laukhin, P. A. Kononovich, M. V. Kartsovnic, A. V. Zvarykina, and L. I. Bubarov, *Pis'ma Zh. Eksp. Teor. Fiz.* **39**, 12 (1984) [*JETP Lett.* **39**, 12 (1984)].
- ⁵S. Söderholm, B. Loppinet, and D. Schweitzer, *Synth. Met.* **62**, 187 (1994).
- ⁶S. Söderholm, B. Loppinet, and D. Schweitzer, *Synth. Met.* **65**, 65 (1994).
- ⁷S. Söderholm, P. R. Varekamp, and D. Schweitzer, *Phys. Rev. B* **52**, 9629 (1995).
- ⁸R. Liu, H. Ding, J. C. Campuzano, H. H. Wang, J. M. Williams, and K. D. Carlsson, *Phys. Rev. B* **51**, 6155 (1995).
- ⁹R. Liu, H. Ding, J. C. Campuzano, H. H. Wang, J. M. Williams, and K. D. Carlsson, *Phys. Rev. B* **51**, 13 000 (1995).
- ¹⁰K. Bender, I. Hennig, D. Schweitzer, K. Dietz, H. Endres, and H. J. Keller, *Mol. Cryst. Liq. Cryst.* **108**, 359 (1984).
- ¹¹U. O. Karlsson, J. N. Andersen, K. Hansen, and R. Nyholm, *Nucl. Instrum. Methods A* **282**, 553 (1989).
- ¹²L. Zuppiroli, in *Low-Dimensional Conductors and Superconductors*, Vol. 155 of *NATO Advanced Studies Institute Series B: Physics*, edited by D. Jérôme and L. G. Caron (Plenum Press, New York, 1987), pp. 301–333.
- ¹³G. Gensterblum, J.-J. Pireaux, P. A. Thiry, R. Caudano, T. Buslaps, R. L. Johnson, G. Le Lay, V. Aristov, R. Günther, A. Taaleb-Ibrahimi, G. Indlekofer, and Y. Petroff, *Phys. Rev. B* **48**, 14 756 (1993).
- ¹⁴W. D. Grobman and E. E. Koch, in *Photoemission in Solids*, Vol. 2, edited by L. Ley and M. Cardona (Springer, Berlin, 1979), pp. 261–298.
- ¹⁵W. D. Grobman, R. A. Pollak, D. E. Eastman, E. T. Maas, Jr., and B. A. Scott, *Phys. Rev. Lett.* **32**, 534 (1974).
- ¹⁶P. Nielsen, *Phys. Rev. B* **10**, 1673 (1974).
- ¹⁷N. Sato, H. Inokuchi, and I. Shirovani, *J. Chem. Phys.* **60**, 327 (1980).
- ¹⁸S. Hino, K. Matsumoto, H. Yamakado, K. Yakushi, and H. Kuroda, *Synth. Met.* **32**, 301 (1989).
- ¹⁹G. K. Wertheim, *Phys. Rev. B* **51**, 10 248 (1995).
- ²⁰B. K. Vainshtein, *Modern Crystallography I* (Springer, Berlin, 1981), Chap. 4.
- ²¹P. Nielsen, A. J. Epstein, and D. J. Sandman, *Solid State Commun.* **15**, 53 (1974); P. Nielsen, D. J. Sandman, and A. J. Epstein, *ibid.* **17**, 1067 (1975).

- ²²D. Schmeiße, K. Graf, W. Göpel, J. U. von Schütz, P. Erk, and S. Hünig, *Chem. Phys. Lett.* **148**, 423 (1988).
- ²³D. Schmeiße, A. Gonzales, J. U. von Schütz, H. Wachtel, and H. C. Wolf, *J. Phys. I (France)* **1**, 1347 (1991).
- ²⁴D. Schmeiße, W. Göpel, U. Langohr, J. U. von Schütz, and H. C. Wolf, *Synth. Met.* **41-43**, 1805 (1991).
- ²⁵D. Schmeiße, W. Jaegermann, Ch. Pettenkoffer, H. Wachtel, A. Jimenez-Gonzales, J. U. von Schütz, H. C. Wolf, P. Erk, H. Meixner, and S. Hünig, *Solid State Commun.* **81**, 827 (1992).
- ²⁶I. H. Inoue, A. Kakizaki, H. Namatame, A. Fujimori, A. Kobayashi, R. Kato, and H. Kobayashi, *Phys. Rev. B* **45**, 5828 (1992).
- ²⁷I. H. Inoue, M. Watanabe, T. Kinoshita, A. Kakizaki, R. Kato, A. Kobayashi, H. Kobayashi, and A. Fujimori, *Phys. Rev. B* **47**, 12 917 (1993).
- ²⁸A. Tanaka, A. Chainani, T. Miura, T. Takahashi, T. Miyazaki, S. Hasegawa, and T. Mori, *Solid State Commun.* **93**, 1 (1995).
- ²⁹B. Dardel, D. Malterre, M. Grioni, P. Weibel, Y. Baer, J. Voit, and D. Jérôme, *Europhys. Lett.* **24**, 687 (1993).
- ³⁰B. Dardel, D. Malterre, M. Grioni, P. Weibel, Y. Baer, and F. Lévy, *Phys. Rev. Lett.* **67**, 3144 (1991).
- ³¹H. J. Schulz, *Int. J. Mod. Phys.* **5**, 57 (1991).
- ³²D. Purdie, I. R. Collins, H. Berger, G. Margaritondo, and B. Reihl, *Phys. Rev. B* **50**, 12 222 (1994).
- ³³R. Claessen, R. O. Anderson, J. W. Allen, C. G. Olson, C. Janowitz, W. P. Ellis, S. Harm, M. Kalning, R. Mancke, and M. Skibowski, *Phys. Rev. Lett.* **69**, 808 (1992).
- ³⁴B. Dardel, M. Grioni, D. Malterre, P. Weibel, Y. Baer, and F. Lévy, *Phys. Rev. B* **45**, 1462 (1992); **46**, 7407 (1993); *J. Phys. Condens. Matter* **5**, 6111 (1993).
- ³⁵Y. Hwu, P. Alméras, M. Marsi, H. Berger, F. Lévy, M. Grioni, D. Malterre, and G. Margaritondo, *Phys. Rev. B* **46**, 13 624 (1992).
- ³⁶M. Nakamura, A. Sekiyama, H. Namatame, A. Fujimori, H. Yoshihara, T. Ohtani, A. Misu, and M. Takano, *Phys. Rev. B* **49**, 16 191 (1994).
- ³⁷C. Coluzza, H. Berger, P. Alméras, F. Gozzo, G. Margaritondo, G. Indlekofer, L. Forro, and Y. Hwu, *Phys. Rev. B* **47**, 6625 (1993).
- ³⁸S. Kagoshima, H. Nagasawa, and T. Sambongi, *One-Dimensional Conductors* (Springer, Berlin, 1988).
- ³⁹N. Toyota, E. W. Fenton, T. Sasaki, and M. Tachiki, *Solid State Commun.* **72**, 859 (1989); N. Toyota and T. Sasaki, *Synth. Met.* **41-43**, 2235 (1991) and F. L. Pratt, J. Singleton, M. Kurmoo, S. J. R. M. Spermon, W. Hayes, and P. Day, *Physics and Chemistry of Organic Superconductors*, Proceedings of the ISSP International Symposium, Tokyo, Japan, 28–30 August 1989 (Springer, Berlin, 1990), p. 200.
- ⁴⁰P. W. Anderson, *A Career in Theoretical Physics* (World Scientific, Singapore, 1994), p. 657–672.
- ⁴¹R. Hlubina, *Phys. Rev. B* **50**, 8252 (1994).
- ⁴²A. Virosztek and J. Ruvalds, *Phys. Rev. B* **42**, 4064 (1990); **43**, 5498 (1991).
- ⁴³F. D. M. Haldane (unpublished) has suggested that long range interactions can give rise to a two-dimensional Luttinger liquid, see also: A. Luther, *Phys. Rev. B* **19**, 320 (1979); A. Houghton and J. B. Marston, *ibid.* **48**, 7790 (1993).
- ⁴⁴P. Kopietz, J. Hermisson, and K. Schönhammer, *Phys. Rev. B* **52**, 10 877 (1995); P. Kopietz and K. Schönhammer, *Z. Phys. B.* **100**, 159 (1996).
- ⁴⁵T. Sasaki, H. Sato, and N. Toyota, *Solid State Commun.* **76**, 507 (1990).
- ⁴⁶K. Kanoda, K. Kato, A. Kawamoto, K. Oshima, T. Takahashi, K. Kikuchi, K. Saito, and I. Ikemoto, *Synth. Met.* **55-57**, 2309 (1993).
- ⁴⁷M. Kurmoo, M. A. Green, P. Day, C. Bellito, G. Staulo, F. L. Pratt, and W. Haynes, *Synth. Met.* **55-57**, 2380 (1990).
- ⁴⁸T. Kouno, T. Osada, M. Hasumi, S. Kagoshima, N. Miura, M. Oshima, H. Mori, T. Nakamura, and G. Saito, *Synth. Met.* **55-57**, 2425 (1993).
- ⁴⁹T. Mori, H. Inokuchi, H. Mori, S. Tanaka, M. Oshima, G. Saito, *J. Phys. Soc. Jpn.* **59**, 2624 (1990).
- ⁵⁰T. Ojiro, K. Kajitani, Y. Nishio, H. Kobayashi, A. Kobayashi, R. Kato, and Y. Iye, *Synth. Met.* **55-57**, 2268 (1993).
- ⁵¹H. Mori, I. Hirabayashi, S. Tanaka, T. Mori, H. Inokuchi, K. Oshima, and G. Saito, *Synth. Met.* **55-57**, 2443 (1993).
- ⁵²W. Y. Chiang, Y. N. Xu, Y. C. Jean, and Y. Lou (unpublished).
- ⁵³J. Voit, *Phys. Rev. B* **47**, 6740 (1993).
- ⁵⁴T. M. J. Emge, P. C. W. Leung, M. A. Beno, H. H. Wang, and J. M. Williams, *Mol. Cryst. Liq. Cryst.* **138**, 393 (1986).
- ⁵⁵T. Mori, A. Kobayashi, Y. Sasaki, H. Kobayashi, G. Saito, and H. Inokuchi, *Chem. Lett.* 957 (1984).
- ⁵⁶J. J. Yeh and I. Lindau, *At. Data Nucl. Data Tables* **32**, 1 (1985).
- ⁵⁷R. Lazzaroni, M. Lögdlund, S. Stafström, W. R. Salaneck, and J. L. Brédas, *J. Chem. Phys.* **93**, 4433 (1990).
- ⁵⁸P. Bätz, D. Schmeiße, and W. Göpel, *Phys. Rev. B* **43**, 9178 (1991).
- ⁵⁹M. P. Keane, A. Naves de Brito, N. Correia, S. Svensson, L. Karlsson, B. Wannberg, U. Gelius, S. Lunell, W. R. Salaneck, M. Lögdlund, D. B. Swanson, and A. G. MacDiarmid, *Phys. Rev. B* **45**, 6390 (1992).
- ⁶⁰Y. F. Miura, A. Kasai, T. Nakamura, H. Komizu, M. Matsumoto, and Y. Kawabata, *Mol. Cryst. Liq. Cryst.* **196**, 161 (1991).
- ⁶¹M. Yoshimura, H. Shigekawa, H. Yamochi, G. Saito, Y. Saito, and A. Kawazu, *Phys. Rev. B* **44**, 1970 (1991).